

^{99m}Tc-Labeled Nanobodies: A New Type of Targeted Probes for Imaging Antigen Expression

Virna Cortez-Retamozo^{1,2}, Tony Lahoutte³, Vicky Caveliers*³, Lea Olive Tchouate Gainkam³, Sophie Hernot^{1,3}, Ann Packeu^{1,3}, Filip De Vos⁴, Chris Vanhove³, Serge Muyldermans^{1,2}, Patrick De Baetselier^{1,2} and Hilde Revets^{1,2}

¹Laboratory of Cellular and Molecular Immunology, Vrije Universiteit Brussel, Brussels, Belgium

²Department of Molecular and Cellular Interactions, VIB, Brussels, Belgium

³In vivo Cellular and Molecular Imaging Laboratory, Vrije Universiteit Brussel, Brussels, Belgium

⁴Department of Radiopharmacy, Ghent University Hospital, Ghent, Belgium

Abstract: Introduction: The development of specific radiolabeled probes towards molecular markers *in vivo* has gained interest as targeted imaging allows for a more accurate detection of diseases. We investigate the feasibility of targeted imaging of cancer antigens using the variable domain of single chain camelid antibodies (Nanobodies[®]) labeled with ^{99m}Technetium. Nanobodies against carcinoembryonic antigen (CEA) were used as a model.

Methods: His₆-CEA1 Nanobodies were generated and labeled with ^{99m}Tc at their His-tag using Tc(I)-tricarbonyl (Isolink, Mallinckrodt, B.V., Petten, The Netherlands). The normal biodistribution was assessed in healthy athymic mice by *ex vivo* analysis at 1 and 3 h. *In vivo* targeting was evaluated in the same mouse model bearing the CEA-positive LS174T tumour or a CEA-negative A431 (human skin carcinoma) control tumour. Pinhole SPECT imaging was performed at 3 hours after intravenous injection of 90 MBq ^{99m}Tc-His₆-CEA1 using a dual-headed gamma camera equipped with pinhole collimators.

Results: Radiolabeling efficiency was > 95%. General biodistribution showed intense renal uptake and marked liver accumulation. Using pinhole-SPECT, the average uptake of ^{99m}Tc- His₆-CEA1 in LS174T (CEA positive) was significantly higher compared to the A431 (CEA negative) control tumour: respectively 3.2 ± 0.6 %IA/cm³ and 1.1 ± 0.2 %IA/cm³ (p < 0.05).

Conclusion: This study presents effective labeling of Nanobodies with ^{99m}Tc using Tc(I)-carbonyl chemistry and shows their potential as a new type of specific probes for imaging antigen expression.

Keywords: Nanobody, carcinoembryonic antigen, Tc(I)-carbonyl chemistry, imaging, tumor targeting.

INTRODUCTION

Molecular imaging is an emerging field in nuclear oncology. This technology is based on the assumption that diseased or injured cells demonstrate a distinctive "pathotype" or signature pattern of altered expression or processing of gene products, which could serve as attractive targets for imaging agents. Next to the transporter-substrate and receptor-ligand models, the antigen-antibody model received much attention and the antigen-binding specificity displayed by antibodies is actively being pursued as a way to target radionuclides for predictive imaging and targeted radiotherapy of cancer [1,2]. Diagnostic antibodies are now commercially available for imaging including ¹¹¹In-satumomab pentetide (Oncoscint) targeting the mucin-like surface glycoprotein TAG-72, and ¹¹¹In-capromab (Prostascint) targeting the prostate-specific membrane antigen. Recently, the Food and Drug Administration (FDA) approved the anti-CD20 mAbs Bexxar (¹³¹I-tositumomab) and Zevalin (⁹⁰Y-ibritumomab tiuxetan) for radioimmunotherapy of non-Hodgkin's lymphoma. Experience with whole antibody imaging and therapy has met with several difficulties due to the intrinsic properties of the antibodies, in particular their clearance kinetics. Since IgG molecules are slowly cleared from the blood pool and the body, the radiolabeled conjugate can cause significant irradiation and toxicity to normal organs with slow diffusion into the tumors, and leads to high background levels in diagnostic scans [3]. Chemical cleavage of monoclonal antibodies to faster clearing Fab molecules has led to diagnostic agents such as the anti-carcinoembryonic antigen (CEA) arcitumomab (CEAScan), that exhibit more favorable pharmacokinetic properties than intact mAbs but are still amenable for improvement [4]. Recombinant approaches have been used to modify several characteristics of monoclonal antibodies to optimize them for *in vivo* targeting [5,6]. Engineered fragments are produced demonstrating rapid uptake into tumor and fast clearance from blood

and non-targeted tissues, characteristics of utmost importance for an imaging agent [6]. Mono-, di-, and tetravalent miniantibodies have been evaluated for *in vivo* targeting in tumor xenograft bearing mice [6-8]. Multimeric fragments have proven superior tumor uptake to those of their scFv counterparts and retain rapid blood clearance, leading to high tumor to blood ratios 24 h post administration. The minibody T84.66 (80 kDa) [9], diabody C6.5 (52 kDa) [10] and T84.66 scFv-Fc (105 kDa) [11] fusion proteins demonstrated even higher tumor uptake; localization is improved because of their longer serum half-life, allowing longer exposure of the target tissue to the antibody fragment. However, suitable tumor to control ratios for optimal contrast can only be obtained after longer intervals between administration and image acquisition, becoming the trade off of these formats.

Nanobodies[®] are a new class of therapeutics based on the single variable region of naturally-occurring antibodies that lack a light chain [12] Fig. (1)[†]. These entities are strictly monomeric, very stable and highly soluble. The unique and well-characterised properties enable Nanobodies to excel conventional therapeutic antibodies and antibody fragments in terms of recognizing hidden or uncommon epitopes, binding to active sites or into cavities of protein targets, tailoring of half-life, drug format flexibility and ease of manufacture [13]. We previously showed that a Nanobody with specificity against lysozyme effectively targeted bulky tumors and metastatic lesions transgenic for hen egg white lysozyme [14]. Although the small size of the Nanobody (15 kDa) resulted in rapid systemic elimination ($T_{1/2\beta}$ = 1.5 hours), mainly *via* renal clearance, the tumor uptake and retention of the Nanobody combined with its clearance kinetics resulted in tumor levels (2.65% IA/g) surpassing those in blood (0.72% IA/ml) as early as 2 hours post administration. These data suggested that Nanobodies could also be effective agents for radioimmunotherapy of cancer. In this study we examine the *in vivo* tumor targeting potential of ^{99m}Tc-labeled Nanobodies using carcinoembryonic antigen (CEA) expression as a model. The

*Address correspondence to this author at the *In vivo* Cellular and Molecular Imaging Laboratory, Vrije Universiteit Brussel, Brussels, Belgium, Laarbeeklaan 101, 1090 Brussels; Tel: +32-2-4775020; Fax: +32-2-4775017; E-mail: vickycaveliers@scarlet.be

[†] Nanobody is a registered trademark of Ablynx N.V.

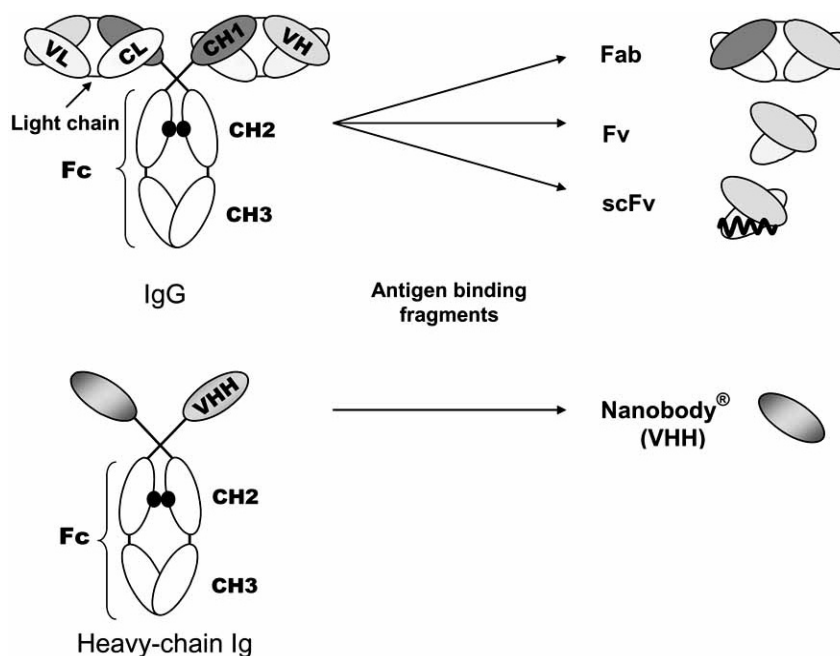


Fig. (1). Schematic representation of different antibody formats, showing intact “conventional” IgG molecules alongside camelid heavy chain antibodies. A variety of antibody fragments are depicted, including Nanobodies, Fab, Fv and scFv.

Nanobodies were radiolabeled with ^{99m}Tc using $^{99m}\text{Tc}(\text{I})$ -tricarbonyl chemistry.

MATERIALS AND METHODS

Nanobody Cloning, Expression and Characterization

Isolation of CEA1 Nanobody was previously described [15]. The genes encoding these Nanobodies were re-cloned as *SfiI-BstEII* fragments in expression vector pAX15 to contain a carboxyterminal hexahistidine tail. The antibody fragments were purified from periplasmic fractions [16] using immobilized metal affinity chromatography (IMAC) on Ni-NTA resin (Qiagen) followed by gel filtration on Superdex 75 HR 16/30 (Pharmacia, Gaithersburg, MD).

The binding characteristics of CEA1 Nanobody were measured by surface plasmon resonance with BIAcore3000 on immobilized antigen as previously described [17]. Nanobody melting curve measurements were carried out with JM-715 spectropolarimeter (Jasco, Japan). The Nanobody melting curves were recorded in the range from 30°C to 90°C with a temperature gradient of 1°C/min at fixed wavelength of 203 nm (the optimal wavelength to monitor the thermally induced unfolding).

^{99m}Tc -Labeling of Nanobodies

Synthesis of [$^{99m}\text{Tc}(\text{CO})_3(\text{H}_2\text{O})_3$] $^+$

To a commercial kit (IsoLink[®], Mallinckrodt Medical B.V., Petten, The Netherlands) containing the following lyophilised formulation: 8.5 mg sodium tartrate, 2.85 mg sodium tetraborate, 7.15 mg sodium carbonate, and 4.5 mg sodium boranocarbonate, 1 ml of fresh $^{99m}\text{TcO}_4^-$ eluate from a $^{99}\text{Mo}/^{99m}\text{Tc}$ generator (Drytec, GE Healthcare, UK) was added (740 MBq – 3.7 GBq). The vial was placed in a boiling water bath for 20 min. After cooling to room temperature, 125 μl of 1N HCl was added to neutralize the solution and decompose any residual boranocarbonate.

Histidine-tag Specific ^{99m}Tc -Labeling of Nanobodies [18]

A 50 μl aliquot of the His₆-CEA1 (1.1-2 mg/ml) was diluted with 50 μl carbonate buffer pH 8.0 and 37-740 MBq ^{99m}Tc -tricarbonyl

solution was added (up to 500 μl). The reaction mixture was heated to 52°C during 1 h. Labeling yield was controlled by Instant Thin Layer Chromatography (ITLC) using glass baked silica gel impregnated glass fiber plates (Pall Corporation, Life Sciences) with 100 % acetone as mobile phase and monitored for 6 h. ITLC chromatograms were monitored with a chromatogram scanner (Veenstra, the Netherlands). If necessary, the radiolabeled Nanobody was further purified with Sephadex G25 disposable columns (NAP-5, GE Healthcare).

Cell Lines and Culture Conditions

The human colon adenocarcinoma cell line LS174 T was obtained from ATCC (Manassas, VA). LS174 T is a trypsinized variant of the LS 180 colon adenocarcinoma cell line and produces large amounts of CEA. Cells were cultured in EMEM media (Gibco BRL, Grand Island, NY) supplemented with 10% heat-inactivated fetal bovine serum, 2 mM L-glutamine, 1mM sodium pyruvate, 1mM non-essential amino acids, 100 units/ml penicillin and 0.1 mg/ml streptomycin. A431 cells, an EGFR overexpressing epidermoid cancer cell line, were kindly provided by Dr. R. Roovers (University of Utrecht, Utrecht, The Netherlands). A431 cells do not express CEA and are used as negative control. Cells were cultured in DMEM (Gibco BRL, Grand island, NY) supplemented with 10% heat-inactivated fetal bovine serum, 2 mM L-glutamine, 1mM sodium pyruvate, 1mM non-essential amino acids, 100 units/ml penicillin and 0.1 mg/ml streptomycin. Cells were grown in mono-layer in Falcon tissue culture dishes (Becton Dickinson, Franklin Lakes, NJ) and incubated at 37°C in humidified incubator with 5% CO₂, 95% air. Cells were detached by using trypsin-EDTA in PBS.

Animal Models

Tumors were grown in the right hind limb region of *nu/nu* nude mice after subcutaneous injection of 5.10⁶ LS174 T (CEA positive) or A431 (CEA negative) cells. Tumors were allowed to grow upto 250-350 mm³. The study protocol was approved by the ethical committee for animal studies of our institution and National Institutes of Health principles of laboratory animal care (NIH publication 86-23, revised 1985) were followed.

Ex Vivo Biodistribution

A total of seven nu/nu mice were analysed for the assessment of the normal biodistribution pattern of CEA-specific Nanobody. Each animal received an intravenous injection of 50 MBq ^{99m}Tc-His₆-CEA1 Nanobody. After euthanasia at 1h (3 animals) or 3h (4 animals) all major organs and tissues were dissected, washed, weighted and counted against a standard of known activity using a gamma counting system (Cobra Inspector 5003, Canberra, Packard). The amount of radioactivity in the organs is expressed as a percentage of the injected activity per gram organ or tissue.

Pinhole SPECT Imaging

3D imaging was performed in nu/nu mice bearing LS174T human colon carcinoma (CEA positive tumor, n=11) and A431 skin carcinoma (CEA negative tumor, n=3). Mice were injected with on average 90 MBq ^{99m}Tc-His₆-CEA1 (10 μg in 100 μl) in the tail vein. At 3 hours after injection of mice were anesthetized with a mixture of 18.75 mg/kg ketamine hydrochloride (Ketamine 1000®, CEVA, Brussels, Belgium) and 0.5 mg/kg medetomidin hydrochloride (Domitor®, Pfizer, Brussels, Belgium). Pinhole SPECT images were acquired using a dual-headed gamma camera (e.cam 180, Siemens) equipped with pinhole collimators (1.5 mm pinhole opening, 64x64 matrix, 64 steps of 20s over 360° rotation). The SPECT images were reconstructed by an interactive reconstruction algorithm adapted for pinhole (pH OS-EM) [19]. For image analysis 3D regions of interest (ROIs) were drawn around the tumor activity (including pixels > 25% of the maximum pixel value) and the injection site using AMIDE software [20]. The counts measured at the injection site were subtracted from the total body counts in case of a difficult injection. Additional ROI's were drawn in liver, kidney, muscle and around the total (including all pixels). A Pinhole SPECT acquisition of a standard was performed as a reference for quantification. Tracer uptake in the tumour and tissues is expressed as % injected activity/cm³ (%IA/cm³) ± standard error. Unpaired t-test of the tumour uptake data was performed. Differences were considered significant when *p* < 0.05.

RESULTS

Nanobody Characterization and Labeling

His₆-CEA1 was purified from bacterial periplasmic extracts by IMAC, followed by size exclusion chromatography (SEC). The use of this two-step purification scheme resulted in the production of homogeneous preparations of the Nanobody with >95% purity. Characterization of kinetic binding parameters of His₆-CEA1 resulted in an affinity constant (K_D) of 7.6 nM with an association rate of 5.27x10⁴ M⁻¹.sec⁻¹ and dissociation rate of 4.04x10⁻⁴ M⁻¹. The Nanobodies also proved to be thermally stable as the heat-induced unfolding revealed melting temperatures of 60°C for His₆-CEA1. ITLC analysis showed a labeling yield > 95 %. Stability of the tracer was confirmed up to 6 h after labeling.

Ex Vivo Biodistribution Analysis

^{99m}Tc-His₆-CEA1 radioactivity distribution over the different organs and tissues is presented in Table 1. The overall biodistribution pattern shows both liver and kidney clearance and some retention in spleen and lungs. Uptake in other organs and blood is minimal.

Pinhole SPECT Imaging

The *in vivo* biodistribution of ^{99m}Tc-His₆-CEA1 in tumour bearing mice as quantified on the images corresponds well with what was found upon dissection, with on average 18.8 ± 2.3 %IA/cm³ in the liver and 71.2 ± 7.9 %IA/cm³ in the kidneys. The total body tracer retention at 3h post injection was 95.8 ± 4.5 %, indicating only limited tracer elimination from the body. The blood activity at 3h was low: 0.5% ± 0.1 % IA/g. The average uptake in the LS174T tumour

was 3 fold higher compared to the CEA negative tumour: 3.2 ± 0.6 %IA/cm³ versus 1.1 ± 0.2 %IA/cm³ respectively. This significant difference (*p*<0.05) confirms the specificity of ^{99m}Tc-His₆-CEA1 for the targeted tumour. The tumour to muscle ratio was 10.7 ± 3.2 for LS174T and 1.7 ± 0.3 for A431, showing an excellent contrast between the CEA positive tumour and the contra-lateral muscle region Fig. (2).

Table 1. Ex Vivo Biodistribution Analysis of ^{99m}Tc-His₆-CEA1 Nanobody in Healthy nu/nu Mice at 1 and 3 Hours p.i.

Organs	1h pi (n=3)	3h pi (n=4)
Brain	0.03 ± 0.01	0.02 ± 0.005
Lungs	7.81 ± 2.14	4.12 ± 1.32
Spleen	13.49 ± 0.89	15.22 ± 8.45
Liver	17.44 ± 8.20	17.95 ± 4.13
Left kidney	66.43 ± 18.02	63.49 ± 8.11
Right kidney	67.09 ± 17.27	66.95 ± 12.43
Heart	0.33 ± 0.11	0.19 ± 0.04
Muscle	0.07 ± 0.02	0.03 ± 0.01
Intestine	0.36 ± 0.07	0.19 ± 0.03
Blood	0.42 ± 0.18	0.20 ± 0.07

Data are presented as %IA/g ± STDEV.

DISCUSSION

Using CEA antigen expressing cells and CEA specific Nanobodies as a model, we demonstrated excellent *in vivo* targeting of ^{99m}Tc-labeled Nanobodies to a cell membrane protein. The general biodistribution showed both liver and kidney clearance resulting in low blood levels at 3h post injection. Nanobodies constitute a new type of probes among the molecules used for targeted radionuclide imaging (and therapy) based on the antigen-antibody model and are distinct from Fab's, minibodies and scFv [21]. Unique advantages of the Nanobody platform are 1) easy and rapid development, (2) easy and cheap production in bacteria and yeast, (3) high flexibility of drug format, i.e. easy to generate multi-specificity and/or multi-valent single molecule formats, (4) superior stability at 37°C and higher temperatures compared to any fragment derived from conventional antibodies [15, 22] and (5) due to specific hydrophilic mutations, Nanobodies are much less prone to aggregation compared to scFv's [15, 22]. In addition, Nanobodies are well capable of tumour penetration due to their small size and they are low immunogenic, at least in mice, since repeated injections of Nanobody did not induce an anti-Nanobody response [14].

The genetically introduced hexahistidine tag at the C-terminus for purification of the Nanobodies allows easy site-specific labeling with [^{99m}Tc(CO)₃(H₂O)₃]⁺ using an IsoLink kit. Other methods have been described for ^{99m}Tc-labeling of recombinant proteins. Until recently, the majority of available strategies employed were dependent on chemical reduction of existing disulfide bonds between two cysteines or on the presence of free sulfhydryl groups made available by either using a thiol-containing chelator [23] or by genetically engineering a cysteine into the recombinant protein [24, 25]. In Nanobodies, the CDR1 region often contains a conserved Cys which may be tethered to Cys in the N-terminal, middle part or the C-terminal of the CDR3, depending on the location of a naturally introduced somatically Cys present in up to 65% of Nanobody-CDR3. This disulfide bond between the CDR1 and CDR3 region has been shown to stabilize the binding domain of Nanobodies. Additionally, it appears as an important thermodynamic feature in the binding reaction to the antigen [26]. Accordingly, techniques for ^{99m}Tc labeling requiring chemical reduction of disulfide bonds were very likely to reduce the stability and affinity of the Nanobodies under study and thus not used. Previously, attempts to introduce genetically engineered

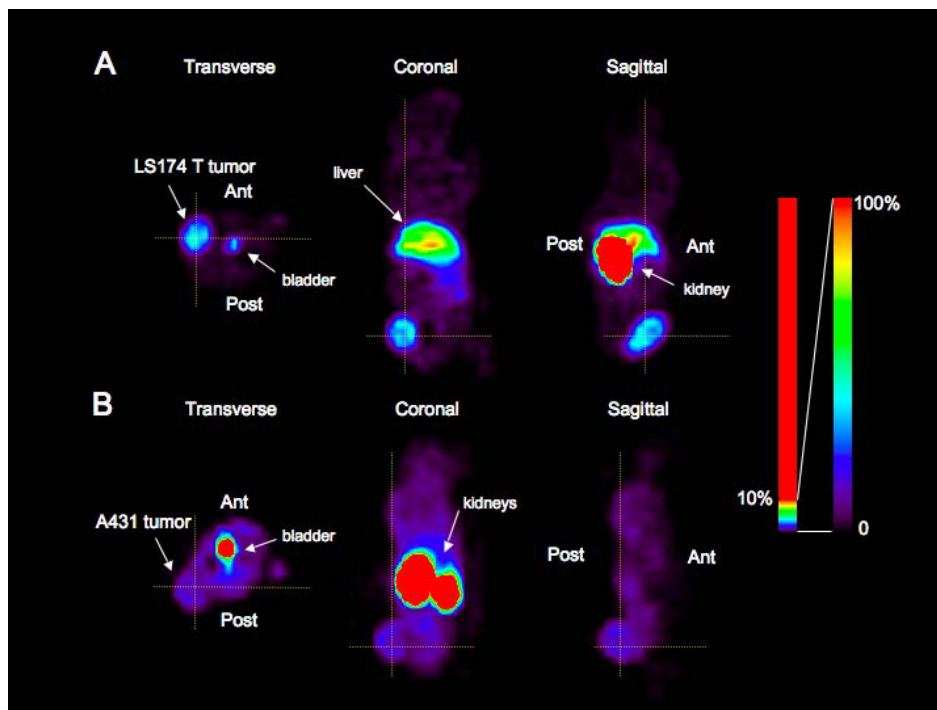


Fig. (2). Pinhole SPECT images of the tumor (transverse, coronal and sagittal slices) at 3 h post injection of ^{99m}Tc -CEA1. A) Mouse carrying the LS174 T human adenocarcinoma xenograft (CEA-positive) on the right thigh. The image is centered on the tumor. Liver uptake can be seen on the coronal view and intense kidney retention is shown on the sagittal view. B) Mouse carrying the A431 epidermoid cancer (CEA-negative). The A431 tumour shows uptake comparable to background. Due to the posterior positioning of the thigh with the tumor, there is no slice through the liver on this image.

cysteine groups into proteins have been shown to lead to problems with protein expression, folding or stability [24,25]. The latter problem has also been associated with trans-chelation methods [27]. Although these problems may be less an issue with Nanobodies, we preferred to use another labeling approach. Interesting about the ^{99m}Tc (I)-tricarbonyl technology [28] is that the incorporation of the radionuclide is directed to the terminal histidine-groups, a site not involved in antigen-binding, and is therefore unlikely to interfere with the antigen-binding properties of the Nanobodies. In agreement, the affinity constant measured by Biacore was confirmed on measurement of the K_D by Scatchard analysis (data not shown). ^{99m}Tc -labeling of ^{99m}Tc -His₆-CEA1 Nanobody at a reaction temperature of 52°C consistently resulted in > 95% incorporation efficiency, avoiding the need for further downstream purification steps. In contrast, ^{99m}Tc -labeling of scFv had to be performed at 37°C and the labeling efficiency ranged from 70%-95%, requiring downstream purification to remove unbound radioactivity. Probably, labeling of scFv at higher temperatures may result in a reduced stability or aggregation, leading to loss of specific binding to the target molecule. A similar observation was made for an anti-HER2 Affibody where ^{99m}Tc -labeling by use of the IsoLink kit at 50°C provided 61% yield and 35% binding to HER2-expressing cells. Increasing the labeling temperature to 70°C provided >90% yield but reduced the cell-binding efficiency to < 4% [29].

As evidenced by the animal experiments, specific tumor uptake of Nanobodies was seen in CEA-positive xenografts and verified by comparison with a control tumor. The 3D pinhole SPECT images offered a superior image quality and resolution and allows for a more accurate tumor delineation. However, the quantification is still susceptible to variability due to inaccuracies in estimating tumor volume when using volume of interest analysis based on including only pixels > 25% of the maximum pixel value. This imprecision can be overcome in future studies with the use of CT-SPECT. A limitation could be the relatively high uptake in liver and kidney, making it difficult to detect lesions inside or close to these organs. The intense signal in the renal cortex suggests glomerular filtration

and reabsorption by the proximal tubuli. Liver uptake could be related to amino acid sequence or the ^{99m}Tc -tricarbonyl complex. ^{99m}Tc labeling through ^{99m}Tc (I)-tricarbonyl has been associated with increased lipophilicity of histidine-tagged Affibodies compared to their radioiodinated analogs [29]. So in order to identify Nanobody imaging agents with the most favourable biodistribution characteristics, also alternative labeling strategies such as radioiodination will be explored. However, since iodine labeling of proteins is usually achieved through lysine or tyrosine moieties, care must be taken with Nanobodies comprising one of these residues in a CDR region in the antigen-binding domain. In addition, experiments with other Nanobodies targeted at different antigens will be interesting to determine whether this biodistribution pattern is typical of all Nanobodies or only valid for the one used here.

CONCLUSION

Site-specific ^{99m}Tc -labeling of Nanobodies is readily achieved using a histidine tag as ligand for $[^{99m}\text{Tc}(\text{CO})_3(\text{H}_2\text{O})_3]^+$. Radiolabeling using a commercial kit in combination with the ease to generate "tailor-made" Nanobodies against a multiplicity of targets, positions these probes as promising imaging agents for profiling the antigen expression in different clinical conditions.

REFERENCES

- [1] Souriau, C.; Hudson, P.J. *Expert. Opin. Biol. Ther.*, **2003**, *3*, 305.
- [2] Jain, M.; Batra, S.K. *J. Nucl. Med.*, **2003**, *44*, 1970.
- [3] Esteban, J.M.; Colcher, D.; Sugarbaker, P.; Carrasquillo, J.A.; Bryant, G.; Thor, A.; Reynolds, J.C.; Larson, S.M.; Schlom, J. *Int. J. Cancer.*, **1987**, *39*, 50.
- [4] Goldenberg, D.M.; Goldenberg, H.; Sharkey, R.M.; Higginbotham-Ford, E.; Lee, R.E.; Swayne, L.C.; Burger, K.A.; Tsai, D.; Horowitz, J.A.; Hall, T.C.; Pinsky, M.; Hansen, H.J. *Cancer Res.*, **1990**, *50*, 909.
- [5] Batra, S.K.; Jain, M.; Wittel, U.A.; Chauhan, S.C.; Colcher, D. *Curr. Opin. Biotechnol.*, **2002**, *13*, 603.
- [6] Wu, A.M.; Yazaki, P.J. *Q. J. Nucl. Med.*, **2000**, *44*, 268.
- [7] Huston, J.S.; George, A.J.; Adams, G.P.; Stafford, W.F.; Jamar, F.; Tai, M.S.; McCartney, J.E.; Oppermann, H.; Heelan, B.T.; Peters, A.M.; Houston, L.L.; Bookman, M.A.; Wolf, E.J.; Weiner, L.M. *Q. J. Nucl. Med.*, **1996**, *40*, 320.

- [8] Willuda, J.; Honegger, A.; Waibel, R.; Schubiger, P.A.; Stahel, R.; Zangemeister-Wittke, U.; Pluckthun, A. *Cancer Res.*, **1999**, *59*, 5758.
- [9] Sundaresan, G.; Yazaki, P.J.; Shively, J.E.; Finn, R.D.; Larson, S.M.; Raubitschek, A.A.; Williams, L.E.; Chatziioannou, A.F.; Gambhir, S.S.; Wu, A.M. *J. Nucl. Med.*, **2003**, *44*, 1962.
- [10] Robinson, M.K.; Doss, M.; Shaller, C.; Narayanan, D.; Marks, J.D.; Adler, L.P.; Gonzalez Trotter, D.E.; Adams, G.P. *Cancer Res.*, **2005**, *65*, 1471.
- [11] Kenanova, V.; Olafsen, T.; Crow, D.M.; Sundaresan, G.; Subbarayan, M.; Carter, N.H.; Ikle, D.N.; Yazaki, P.J.; Chatziioannou, A.F.; Gambhir, S.S.; Williams, L.E.; Shively, J.E.; Colcher, D.; Raubitschek, A.A.; Wu, A.M. *Cancer Res.*, **2005**, *65*, 622.
- [12] Hamers-Casterman, C.; Atarhouch, T.; Muyldermans, S.; Robinson, G.; Hamers, C.; Songa, E.B.; Bendahman, N.; Hamers, R. *Nature*, **1993**, *363*, 446.
- [13] Revets, H.; De Baetselier, P.; Muyldermans, S. *Expert. Opin. Biol. Ther.*, **2005**, *5*, 111.
- [14] Cortez-Retamozo, V.; Lauwereys, M.; Hassanzadeh, Gh.G.; Gobert, M.; Conrath, K.; Muyldermans, S.; De Baetselier, P.; Revets, H. *Int. J. Cancer*, **2002**, *98*, 456.
- [15] Arbabi Ghahroudi, M.; Desmyter, A.; Wyns, L.; Hamers, R.; Muyldermans, S. *FEBS Lett.*, **1997**, *414*, 521.
- [16] Skerra, A.; Pluckthun, A. *Science*, **1988**, *240*, 1038.
- [17] Cortez-Retamozo, V.; Backmann, N.; Senter, P.D.; Wernery, U.; De Baetselier, P.; Muyldermans, S.; Revets, H. *Cancer Res.*, **2004**, *64*, 2853.
- [18] Waibel, R.; Alberto, R.; Willuda, J.; Finnem, R.; Schibli, R.; Stichelberger, A.; Egli, A.; Abram, U.; Mach, J.P.; Pluckthun, A.; Schubiger, P.A. *Nat. Biotechnol.*, **1999**, *17*, 897.
- [19] Vanhove, C.; Defrise, M.; Franken, P.R.; Everaert, H.; Deconinck, F.; Bossuyt, A. *Eur. J. Nucl. Med.*, **2000**, *27*, 140.
- [20] Loening, A.M.; Gambhir, S.S. *Mol. Imaging*, **2003**, *2*, 131.
- [21] Van de Wiele, C.; Revets, H.; Mertens, N. *Q. J. Nucl. Med. Mol. Imaging*, **2004**, *4*, 317.
- [22] Davies, J.; Riechmann, L. *Protein Eng.*, **1996**, *9*, 531.
- [23] Nedelman, M.A.; Shealy, D.J.; Boulin, R.; Brunt, E.; Seasholtz, J.I.; Allen, I.E.; McCartney, J.E.; Warren, F.D.; Oppermann, H.; Pang, R.H.; Berger, H.J.; Weisman, H.F. *J. Nucl. Med.*, **1993**, *34*, 234.
- [24] George, A.J.; Jamar, F.; Tai, M.S.; Heelan, B.T.; Adams, G.P.; McCartney, J.E.; Houston, L.L.; Weiner, L.M.; Oppermann, H.; Peters, A.M. *Proc. Natl. Acad. Sci. USA*, **1995**, *92*, 8358.
- [25] Verhaar, M.J.; Keep, P.A.; Hawkins, R.E.; Robson, L.; Casey, J.L.; Pedley, B.; Boden, J.A.; Begent, R.H.; Chester, K.A. *J. Nucl. Med.*, **1996**, *37*, 868.
- [26] Muyldermans, S. *J. Biotechnol.*, **2001**, *74*, 277.
- [27] Stalteri, M.A.; Bansal, S.; Hider, R.; Mather, S.J. *Bioconjug Chem.*, **1999**, *10*, 130.
- [28] Alberto, R.; Ortner, K.; Wheatley, N.; Schibli, R.; Schubiger, A.P. *J. Am. Chem. Soc.*, **2001**, *123*, 3135.
- [29] Orlova, A.; Nilsson, F.Y.; Wikman, M.; Widstrom, C.; Stahl, S.; Carlsson, J.; Tolmachev, V. *J. Nucl. Med.*, **2006**, *47*, 512.

Received: July 19, 2007

Revised: August 24, 2007

Accepted: August 24, 2007